Atmospheric Environment 45 (2011) 3015–3024

Contents lists available at ScienceDirect

Atmospheric Environment

journal homepage: www.elsevier.com/locate/atmosenv

Quantitative analysis of mineral phases in atmospheric dust deposited in the south-eastern Iberian Peninsula

J.L. Díaz-Hernández [a,*], J.D. Martín-Ramos [b], A. López-Galindo [c]

[a] IFAPA Camino de Purchil, Area de Recursos Naturales, Camino de Purchil s/n, 18080 Granada, Spain
[b] Dpto. Mineralogía y Petrología, UGR, Avda. Fuentenueva s/n, 18002 Granada, Spain
[c] Instituto Andaluz de Ciencias de la Tierra, IACT-CSIC-UGR, Avda. Fuentenueva s/n, 18002 Granada, Spain

ARTICLE INFO

Article history:
Received 24 April 2010
Received in revised form
7 March 2011
Accepted 7 March 2011

Keywords:
Aerosols mineralogy
Dust deposition rates
African dust
Powder X-ray diffraction
Sulphates neoformation

ABSTRACT

Particulate matter suspended in air mainly consists of a complex, multiphase system. Its nature is largely mineral at a global scale, and it has a significant physicochemical impact on the Earth's atmosphere and on biogeochemical cycles. These mineral phases come mainly from windblown soil processes, mostly from great deserts. Despite their importance, the behaviour of their airborne components in time and space is not well known.

This study found that the rate of mineral deposition over an annual cycle in the south-eastern Iberian Peninsula was 26.03 g m^{-2} yr^{-1}, with maxima in spring and summer. Using powder X-Ray diffraction techniques, this value has been broken down as follows (in g m^{-2} yr^{-1}): quartz (4.90), dolomite (3.36), calcite (3.28), micas (2.97), smectites (2.10), halite (1.84), kaolinite (1.82), sulphates (1.28), amorphous matter (1.15), feldspars (0.18) and graphite (0.17). Although quartz normally is the major individual component of solid particles in the atmosphere—carbonates (calcite + dolomite) can exceed quartz, and phyllosilicates can total as much as carbonates. Clay minerals correlate well with salts (sulphates and halite), and there is an antagonistic relation between sulphates and calcite. Amorphous matter consists of a mixture of metal oxides and organic compounds, among others. Graphite, a net anthropogenic constituent of atmospheric dust, only represents minor quantities.

The behavioural differences of the minerals are due to their different reactivity, based on their intrinsic properties of specific surface area, deliquescence, swelling and water retention capacity, and the presence of metallic and exchangeable cations. Smectites seem to play an essential role in the atmospheric processing of SO_2 and in secondary sulphate genesis.

1. Introduction

On a global scale, mineral dust is the major contributor to aerosol loading. Estimated quantifications of global dust emissions vary considerably in the range of 1500–2600 Tg yr^{-1} (IPCC, 2007). This particulate matter plays an important role in atmospheric physicochemical processes and the environment (Dentener et al., 1996; Jacob, 2000), because dust particles provide abundant reaction sites for many heterogeneous reactions involving atmospheric gases. This matter is then incorporated into the marine and terrestrial ecosystems.

Wind soil erosion from certain arid and semi-arid regions is considered to be the principal source of atmospheric dust (Prospero et al., 2002). Anthropogenic sources have been estimated to contribute only 5–7% of total mineral dust (Tegen et al., 2004), but the IPCC (2007) raised this amount to 20%, admitting that methods used to estimate anthropogenic contribution to dust emissions involve large uncertainties.

The major natural source region is North Africa (Goudie, 2009), not only affecting the Iberian Peninsula, but also the entire Mediterranean basin (Tafuro et al., 2006; Gobbi et al., 2007), and contributing significantly to the total atmospheric aerosol load (Andreae, 1995). North Africa accounts for 62% of the total global dust load in the atmosphere (Tanaka and Chiba, 2006). Even though the features of these emissions have been broadly studied (Chester and Johnson, 1971; Glaccum and Prospero, 1980; Middleton and Goudie, 2001, and references therein), only a few studies have actually characterized the dust mineralogy of an area so heavily influenced by Saharan additions as the western Mediterranean, and only for specific cases (Ávila et al., 1997, 1998; Alastuey et al., 2005).

* Corresponding author.
E-mail address: josel.diaz@juntadeandalucia.es (J.L. Díaz-Hernández).

1352-2310/$ – see front matter © 2011 Elsevier Ltd. All rights reserved.
doi:10.1016/j.atmosenv.2011.03.024

The SAMUM'06 project studied the major constituents of the aerosols from southern Morocco in the period 13 May–7 June 2006 (Kandler et al., 2009), obtaining low temporal variability of the bulk mineralogical composition.

To date we do not have precise information on long-term deposition rates of dust and its minerals (Lawrence and Neff, 2009), despite their importance for the understanding of aerosol properties and dust–cloud interaction, their potential importance for heterogeneous chemistry and modelling of atmospheric processes, and their subsequent impact on biogeochemical cycles.

Little is known about heterogeneous SO_2 oxidation as the mechanism of sulphate formation on mineral dusts. Several studies on different natural substrates, such as Saharan dust (Ullerstam et al., 2002, 2003) and Chinese loess (Usher et al., 2002), have examined the kinetics of heterogeneous SO_2 oxidation on these aerosols. Usher et al. (2002) suggested that the uptake coefficient of Chinese loess can be predicted from the reactivity of its individual components along with the average composition of the loess. Al-Hosney and Grassian (2004) and Li et al. (2006) look more closely at several processes and mechanisms of heterogeneous oxidation on calcite surfaces, which are an important component of Asian loess. However, a number of questions have arisen concerning the relative importance of the components of mineral dust and their reaction mechanisms.

The main aim of this study is to determine the yearly airborne mineral flux over the south-western Mediterranean area. To this end, we determined dust additions in the course of a complete year, specifying and quantifying the mineralogical phases involved and subsequently describing some relationships between them. We focussed especially on the impact of African dust and the formation (identification/quantification) of secondary mineral phases.

2. Material and methods

This research covered the course of a complete year, during which both dry deposition (as a naturally occurring, continuous phenomenon from atmosphere to soil), and wet deposition (associated with rain events) were collected. Although records are available for several years, we chose 1992 as the year with the most complete record and sufficient dust quantity to perform an assessment, thus giving a broader view of the evolution of aerosol composition over time in the southern Iberian Peninsula.

2.1. Regional framework

The sampling site is located at 37°10′N–3°31′W, 640 masl (Granada Depression, south-eastern Iberian Peninsula), surrounded by dolomitic limestone and siliceous relief. The soils in the depression are Calcareous Fluvisols (IARA-CSIC, 1989), with irrigated crops within a radius of a few tens of kilometres around the monitoring station and olive groves and forestry further away. The area is not heavily industrialized.

The mean annual temperature is 15.1 °C, ranging from 6.7 to 24.8 °C (January and July, respectively), and mean annual precipitation is 357 mm over the last 30 years, which corresponds to a semi-arid Mediterranean climate (data from Granada airport, Spanish Meteorological Agency, AEMET). The precipitation during the monitoring period was 311.7 mm, distributed in 78 rainy events.

Conventional aerodynamic data show a high annual percentage of calm (approximately 63%), with predominantly gusty winds under 5 km h^{-1} up to 10 AM, followed by an increase up to 20 km h^{-1} around midday, dropping around 4 PM to approximately 0 km h^{-1}. These values minimize the incidence of local supplies to our samplers. The samples collected at this site depict a relatively clean environment, although local sources can be a factor at any site.

2.2. Monitoring and sampling

Monitoring was carried out by collecting the deposited atmospheric dust in dry passive collectors (Díaz-Hernández and Miranda, 1997) once a week, with control of any unexpected incident (spillage, contamination, etc.). Because it rained on 20% of the days in the year, and around 70% of the rainy episodes were lower than 5 mm day^{-1}, losses through splashing were minimal. Medium-sized plastic trays (0.1898 and 0.1380 m^2 surface area and 10 cm deep) were used to obtain quantities suitable for later analysis, and were placed on the roof of a building 8 m high, where local supplies are further reduced by surrounding irrigated land. The dust was carefully collected using a brush (F1 samples) and its characteristics examined under stereo microscope. However, in order to obtain the true deposition rate, collectors were washed with 250 cm^3 of distilled water to remove dust adhered by dew. This suspension was allowed to settle for 24 h, after which the upper 200 cm^3 were removed by pipette and both parts then evaporated, thus obtaining F2 samples (corresponding to the lower 50 cm^3) and F3 samples (upper 200 cm^3). The weekly deposition rate was obtained by adding these three fractions together. Each fraction was weighed on analytical scales (0.1 mg precision) and stored separately in glass vials. As sampling was carried out weekly, the mean rate is expressed in mg m^{-2} d^{-1} for each week. Some missing data were completed by using the closest preceding and following data.

2.3. Qualitative and quantitative analysis by powder X-ray diffraction (PXRD)

The specimens (unground, given that original particle size was <20 μm) were examined using a Philips PW 1710/00 diffractometer, with graphite monochromator, automatic slit, CuKα radiation and on-line computer connection. The specimens were mounted on a zero-background mount (Si plate). Data were collected for 0.4 s integration time in 0.05° 2θ steps at 40 kV and 40 mA, in a 2θ interval between 3 and 70°. Data processing was performed using the XPowder® program in order to obtain the qualitative and quantitative mineral composition (Martín-Ramos, 2004). Additional details of this process can be found in Chapter 6 of the XPowder program's user guide (Martín-Ramos, 2004).

2.4. Electron microscopy techniques

High-resolution transmission electron microscopy (HRTEM) was used with selected samples to obtain morphological and chemical information. Samples were suspended in ethanol, sonicated for 2 min and placed on a Cu grid. These samples were examined using a Phillips CM-20 electron microscope. Point-to-point resolution was 0.27 nm and beam sizes were 100 nm in TEM mode. Quantitative microanalyses were carried out in STEM mode using an EDAX-Genesis system equipped with a Si (Li) detector, using a 7-nm beam diameter and a 20 × 100 nm scanning area. Electron diffraction patterns were obtained from selected areas (SAED) and HRTEM lattice-fringe images were obtained following Buseck et al. (1988).

3. Results

3.1. Features and rates of dust addition

The mineral mass has earthy, sometimes pinkish colours (10YR6/3, Munsell Color Company, 1995). Under stereo microscope it is usually accompanied by soot (carbonaceous spherules and other unidentified blackish residues) and remnants of burnt plants

and other vegetal remains, with occasional vegetal filaments and pollen. No iberulites (microespherules representing aerosols aggregation phenomena, Díaz-Hernández and Párraga, 2008) were found, although there were periods with appropriate conditions, the best being around 2nd March, 15th June and 21st September, close to or coinciding with red rain events.

The dustfall rate during this year for this region was established at 23.06 g m^{-2} yr^{-1} Fig. 1 shows the distribution of the weekly dustfall rates, with maxima occurring during southerly winds (38%), contributing 50% of the total for that year. A similar tendency was found for total suspended particles (TSP) collected during the same period at the nearby ES07 EMEP site, based on daily sampling using a high-volume sampler.

As a general rule, TSP is correlated with bulk deposition (Fig. 1) indicating that an increase in suspended dust accounts for an increase in deposition. This correlation suggests an important contribution of dry deposition. In addition, precipitation events such as those recorded in April cause a marked decrease in levels of TSP and in deposition load. There are some exceptions such as the summer rain events where there is a clear decrease in TSP together with significant deposition load, related to wet scavenging.

3.2. Detected mineralogical phases and development in time

We examined both the certain and the probable/possible mineral phases, on the basis of studies by Glaccum and Prospero (1980), Coudé-Gaussen et al. (1987), Ganor (1991), Ávila et al. (1997), Claquin et al. (1999), Ganor et al. (2000), Falkovich et al. (2001), Reid et al. (2003), Menéndez et al. (2007), and our own observations using electron microscopy. The results obtained by XPowder software (F1, F2 and F3 samples) are included as Supplementary material.

We detected the following mineral phases: bassanite, calcite, chlorite, dolomite, feldspars, graphite, gypsum, halite, kaolinite, illite/muscovite, paragonite, quartz and smectites (13.6, 17.6 and 22.5 Å). Some other minerals classifiable as "trace phases" were identified by TEM: Ti and Al oxides (Fig. 2A, B and D), apatite and, probably, some additional sulphate and carbonate. Palygorskite was only detected in three samples (Fig. 2C), and was not considered in quantification. In addition, some non-classifiable amorphous material is also present.

In general, the mineral phases detected present remarkable continuity over time, with no relevant patterns. Moreover, the mineralogy of each fraction is essentially similar (Fig. 3), although quartz and graphite percentages increased in F1 samples, and amorphous matter, bassanite (and sulphates in general), and halite were mainly concentrated in F3 samples, because they mostly derived from the evaporation of a solution containing dissolved and suspended minerals. To a lesser extent, the same is true for calcite and smectites, considering that calcite partially comes from precipitation and smectites from suspension. Satisfactory diffractograms were not always obtained from F3 samples because of the small amounts of sample available in some cases.

The percentages of the various mineral phases identified (Fig. 4) varied over time in close correlation with the dust rates, a trend that was most noticeable in the main mineral phases, especially quartz.

3.3. Regression analysis

An initial analysis was carried out by considering data from the three types of samples (F1, F2 and F3), although F1 samples seem to better reflect the original relationship among the different minerals. Those found in F2 and F3 are, *a priori*, of less interest because they may have undergone dissolution and subsequent neoformation processes during sample preparation and manipulation, in many cases suffering other milder changes. For comparative purposes, Table 1 includes the most significative correlations found in both F1 samples and all types of samples (F1, F2 and F3).

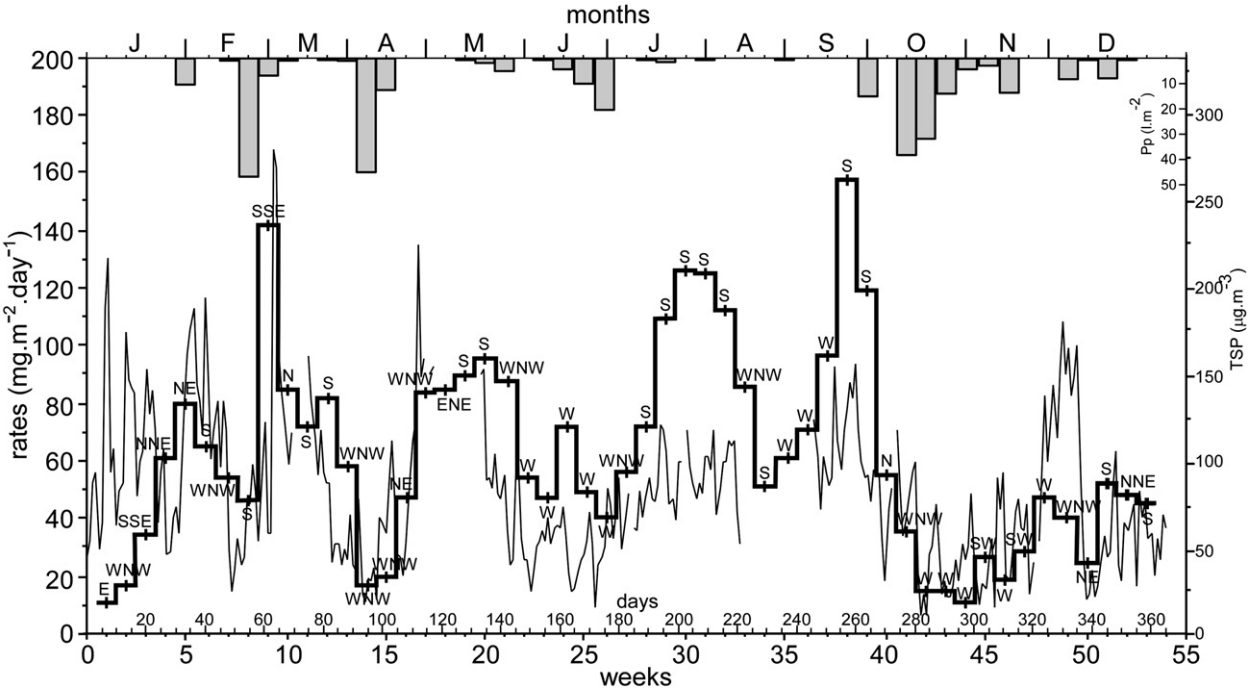

Fig. 1. Temporal distribution of dust additions in the southern Iberian Peninsula. The heavy line indicates weekly atmospheric dust deposition rates (three fractions) and letters designate the predominant wind direction regime. Records of weekly precipitation (Granada airport, AEMET) and daily TSP levels (thin lines) (La Cartuja station, AEMET) are also shown.

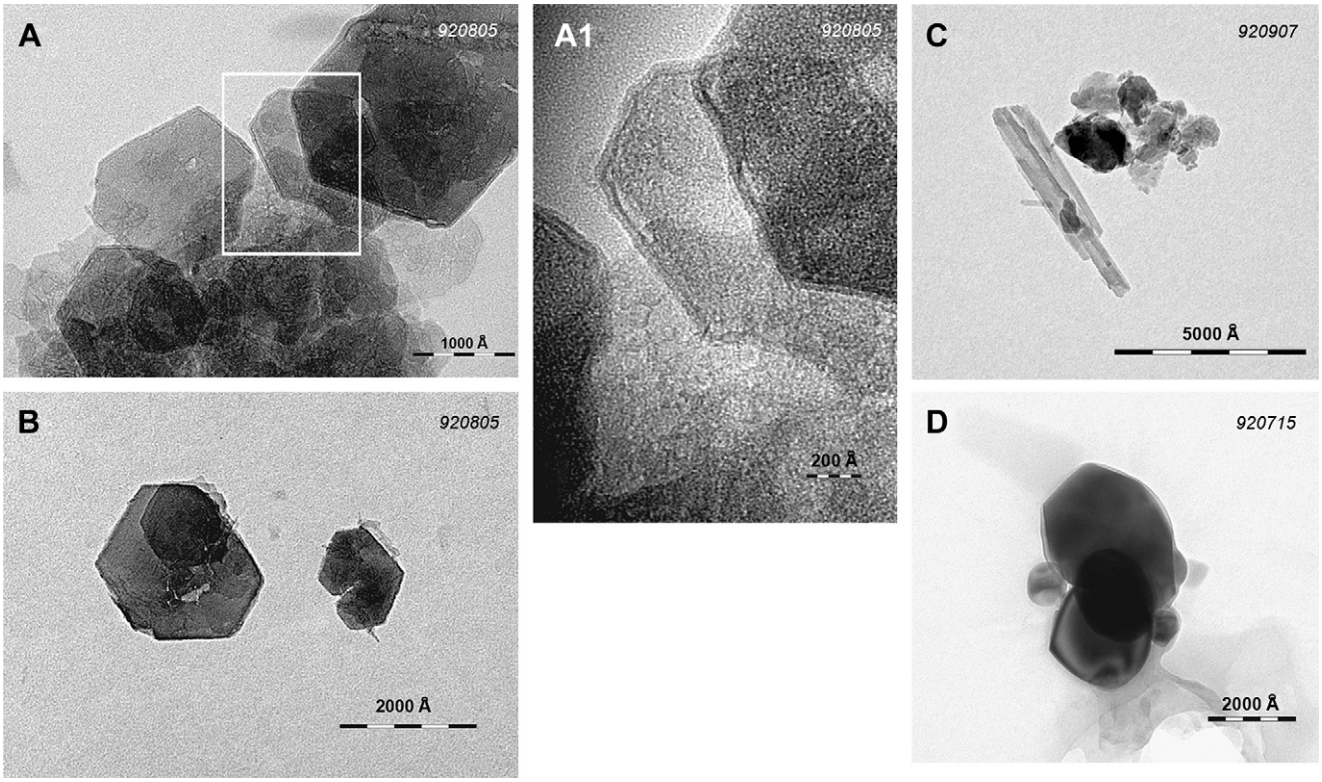

Fig. 2. HRTEM images of some trace minerals found in F1 samples. (A) Aluminium oxyhydroxide (probably gibbsite) with hexagonal flake shapes. (A1) Detail of the previous crystals. (B) Two well individualized crystals of the same mineral. (C) Palygorskite crystal showing an elongated shape. (D) Typical crystal of Ti oxide. The number in the right-hand corner is the sample number, indicating a time key.

The ranges of each mineral and its outliers are shown in Fig. 5. Rainfall on turbulent regimes caused one outlier for calcite and gypsum and two for dolomite and bassanite. The regression analyses did not take these outliers into account. Smectites were included in one group (Sm) and bassanite and gypsum in the sulphates group (Sulph). In general terms, graphite and amorphous matter correlate poorly with most of the minerals, and behave antagonistically to each other. Exceptions to this are the good correlations observed between graphite and quartz and between amorphous matter and halite.

Some of the more significant correlations are represented in Fig. 6, which includes six antagonistic trends (top) and six with a high degree of association (bottom). The most outstanding antagonistic relation is between quartz–salts (halite and sulphates),

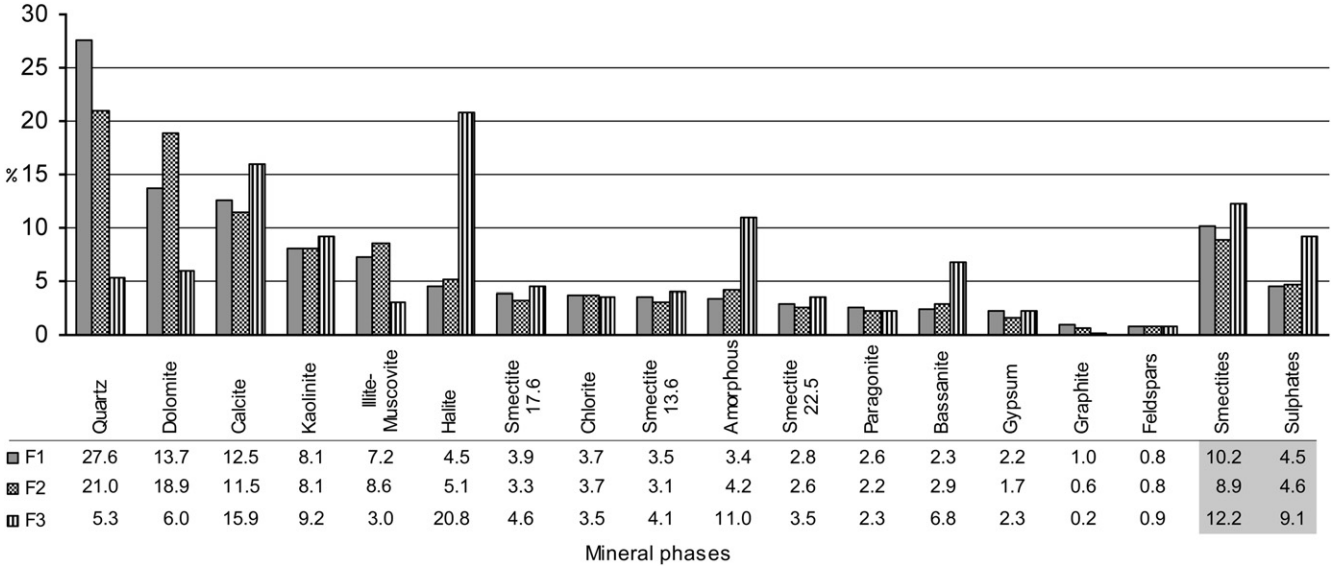

Fig. 3. Average contents of detected mineral phases, in decreasing order, comparing samples F1, F2 and F3. The shadowed area represents "smectites" (Sm), referring to the sum of percentages of minerals with interlaminar spacing at 13.6, 17.6 and 22.5 Å, and "sulphates" (Sulph), consisting of the sum of bassanite and gypsum.

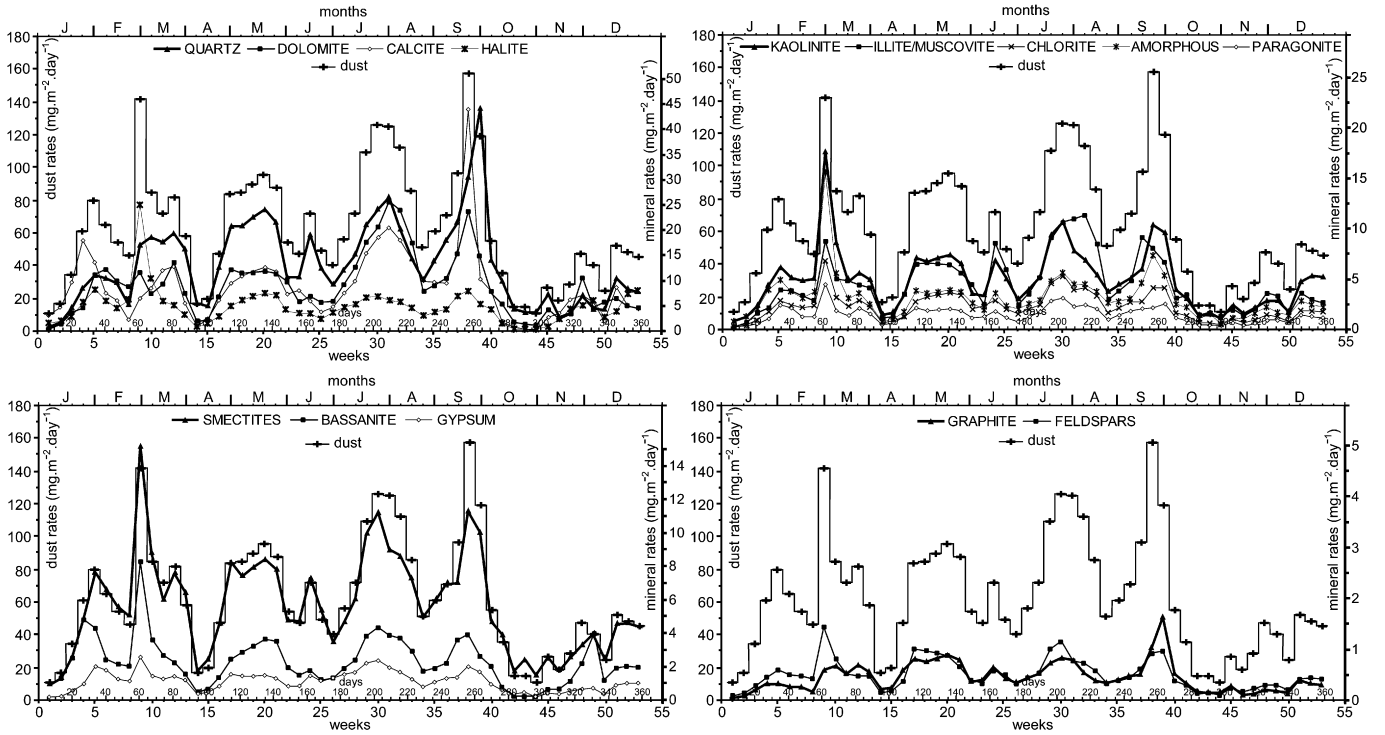

Fig. 4. Evolution in time of mineral rates (mg m^{-2} d^{-1}, data obtained by adding the three fractions), grouping the minerals according to affinity of rate in each inset. In each case the scale of the *Y* (right) axis has been altered to visualize the oscillations throughout the year.

quartz–smectites, and calcite–gypsum. Besides, there is a highly positive correlation between gypsum and smectites and, in general, between sulphates and phyllosilicates other than illite/muscovite. The high correlation between halite and sulphates is also significant.

4. Discussion

The accumulation rate obtained (23.06 g m^{-2} yr^{-1}) falls within the range of those described by Simonson (1995) and Lawrence and Neff (2009) in a global context, and by Loÿe-Pilot et al. (1986), Bücher (1994) and Guerzoni et al. (1997) in the Western Mediterranean area, for periods similar to ours. Our sampling took place during a year with close to average precipitation, and samples were recovered in both dry and wet deposition, in a context distant from the marine boundary layer (MBL). This rate also corresponds well with the TSP concentration. The annual distribution pattern of the rate (Fig. 1) shows a clear tendency of main maxima in summer and spring, and minima in winter and autumn, with a clearly upward trend until the month of September, followed by a sharp drop related with precipitation events.

Local components may have contributed to this accumulation rate, and even if it is difficult to pinpoint their relative proportions in the samples, some considerations can be made. For instance, the outliers of calcite and dolomite appeared on days with rain and strong gusty winds. The correlation between calcite and dolomite is significant and it may indicate a common source for these minerals, such as the calcareous reliefs surrounding the Granada basin. On the other hand, paragonite is absent from the southern Hesperic Massif (Martín-Ramos et al., 1988), but is found in the neighbouring Sierra Nevada and other more distant regions. The good correlation found between paragonite and sulphates suggests a more distal and longer atmospheric process than if this phyllosilicate only came from Sierra Nevada, and thus local additions seem to be small. Celestine could be another index mineral for this (there are large strontium quarries in the Granada depression) but its absence also suggests low local additions.

We classify the mineral phases detected in three groups, according to their mean abundance in the three types of samples (F1, F2 and F3) (Fig. 3):

- Major constituents: quartz, carbonates (dolomite, calcite), illite/muscovite, and kaolinite.
- Minor constituents: chlorides (halite), paragonite, chlorite, smectites (three types), sulphates (bassanite, gypsum), graphite, feldspars and amorphous matter.
- Traces (detected only in some samples or by HRTEM): palygorskite, apatite, titanium oxides, and aluminium oxyhydroxides.

The limit between the two first groups was randomly set at 5%. However, the halite content is usually close to this limit, and the halite, amorphous matter and bassanite in F3 samples were well in excess of this value (Fig. 3). If all smectite types are grouped together, they would as a whole form part of the first group, with amounts similar to calcite; likewise sulphates would be near 5%. So, from the quantitative point of view, smectites should be considered an important component of the aerosols, with a significant influence on the atmospheric processes, given that their properties make them particularly reactive in this medium.

Although the mineral phases detected are consistent with some previous studies (Glaccum and Prospero, 1980; Molinaroli, 1996; Reid et al., 2003; Menéndez et al., 2007; Lawrence and Neff, 2009), the present evaluation reveals some significant facts. Atmospheric graphite comes from anthropogenic activity, as indicated by other authors (Andreae, 2001; Gelencsér, 2004; Kovács-Kis et al., 2006; Adachi and Buseck, 2008), although traditionally little attention has been paid to it. It is a component that was repeatedly observed in the samples analysed, often taking the form of black, porous

Table 1
Significative correlations ($|R| > 0.5$) found using data from F1 samples and from all types of samples (F1, F2 and F3, in bold and italics) based on quantification obtained by the XPowder program. Insets represent the main correlations found between sulphates and phyllosilicates. The shaded area shows how F1 samples present better correlations and these are more numerous when compared to their equivalent (F1, F2 and F3 samples).

	Quartz	Feldspars	Graphite	Calcite	Dolomite	Bassanite	Gypsum	Halite	Total smectites	Chlorite	Illite / Muscovite	Paragonite	Kaolinite	Amorphous	Total sulphates
Quartz	1		***0.900***			***-0.719***		***-0.712***						***-0.640***	***-0.795***
Feldspars		1							***0.532***	***0.534***			***0.627***		
Graphite	0.722		1			***-0.619***		***-0.609***						***-0.557***	***-0.647***
Calcite				1											
Dolomite					1	***-0.507***		***-0.549***			***0.518***			***-0.513***	***-0.589***
Bassanite						1		***0.900***			***-0.542***			***0.536***	***0.938***
Gypsum	-0.639					0.531	1		***0.790***	***0.581***		***0.635***	***0.684***		
Halite	-0.583					0.593	0.716	1			***-0.601***			***0.507***	***0.862***
Total smectites	-0.519	0.500			-0.532	0.632	0.775	0.632	1	***0.625***		***0.612***	***0.774***		
Chlorite		0.541				0.558	0.721	0.574	0.707	1		***0.649***	***0.678***		
Illite / Muscovite											1			***-0.505***	***-0.584***
Paragonite							0.554		0.620	0.657		1	***0.579***		
Kaolinite	-0.571	0.567			-0.555	0.647	0.745	0.688	0.776	0.729		0.571	1		
Amorphous								0.577						1	***0.619***
Total sulphates	-0.620					0.826	0.917	0.770	0.811	0.784		0.564	0.844		1

carbonaceous spherules, occasionally associated with heavy metals. Electron diffraction (HRTEM) examination showed 3.44 Å basal spacing, characteristic of graphite, with low crystallinity and sometimes preferential orientation.

Smectites, the predominant clays, were quantified as belonging to three different types according to their basal spacing at 13.6, 17.6 y 22.5 Å, because *a priori* each of them could show different reactivity in the atmospheric environment. From the correlation with sulphates we observed that the reactivity of the 13.6 Å smectite is somewhat higher than the other two smectites, with a preferential tendency to produce gypsum in SO_2 atmospheric processing ($R = 0.7530$, $p = 0.000$).

Observations have also shown that sulphate species are often found as sulphate coatings on atmospheric dust as a result of cloud processing (Glaccum and Prospero, 1980; Zhuang et al., 1999; Mills et al., 2005; Manktelow et al., 2010); in this sense sulphated phases are neoformed. Actually we can find several possible sulphated phases, although we have only confirmed and evaluated the presence of bassanite and gypsum.

Field measurements showed a correlation between non-sea-salt sulphates and mineral aerosols (Carmichael et al., 1996; Zhang et al., 2000). In our case the correlation between sulphates and smectites is one of the highest we obtained (Table 1). On the contrary, calcite and sulphates are antagonistic. As indicated by Glaccum and Prospero (1980), this antagonistic relationship may be the result of the involvement of calcite in the atmospheric processing of sulphur dioxide: thus, as the gypsum percentage increases, the calcite value decreases. But the case of calcite is different to that of smectites, because the reaction of calcite with sulphuric acid implies destruction of the carbonate to produce gypsum and carbon dioxide. However the reaction of exchangeable calcium from smectites with sulphuric acid cannot destroy the silicate structures, producing sulphates associated to smectite remains.

A clear, close relation between smectites and sulphates has also been observed on iberulites (Díaz-Hernández and Párraga, 2008), whose cores often contain a few calcite grains with no remains of sulphates, concentrated in the smectite rind. It is debatable if the source area of our aerosols also has low calcite content, but the

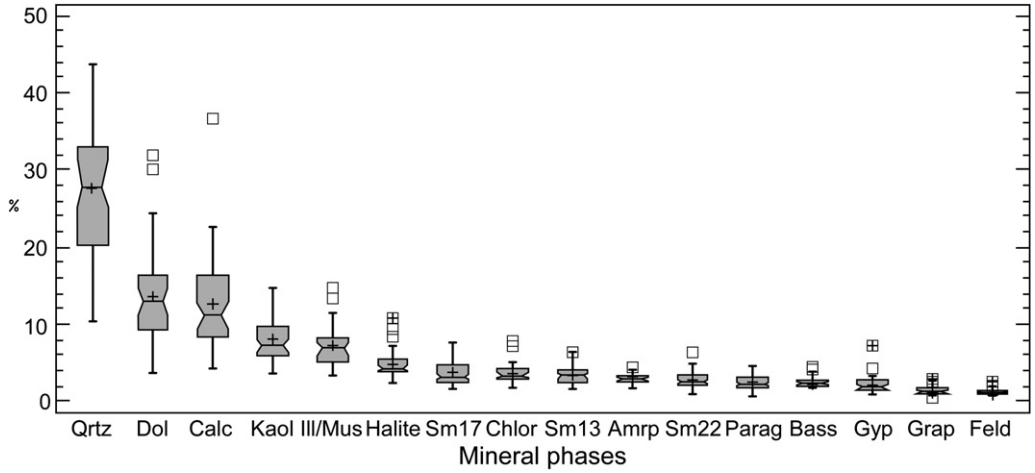

Fig. 5. Statistical characteristics of mineral phases contained in F1 samples.

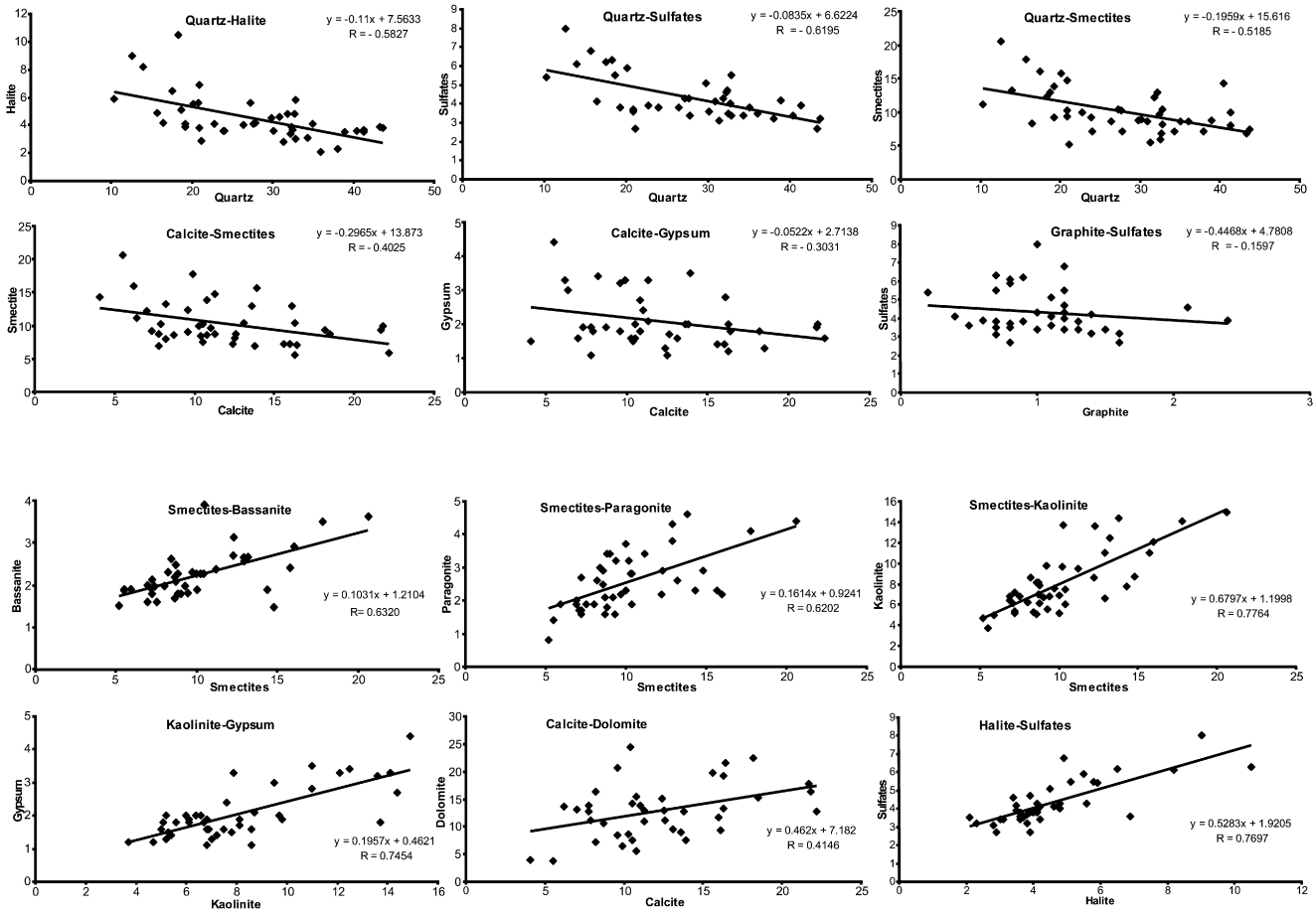

Fig. 6. Notable correlations found in F1 samples. Values on %.

reactivity of calcite compared to smectite is low. This can be explained by several well known facts: the specific surface area of the smectites is very high; their water affinity (deliquescence) is significant; the swelling capacity of smectites allows SO_2 to enter the interlayer, thus increasing the surface area; their structure of honeycombed compartments facilitates water retention; their association with metallic cations (Ti, Fe) as catalyzers in heterogeneous processes (mainly in the transformation of SO_2 to sulphuric acid) is fundamental; and the existence of exchangeable cations (mainly calcium) to ultimately form bassanite/gypsum (Basma et al., 1996; Ullerstam et al., 2003; Meunier, 2005; Dogan et al., 2007; Herich et al., 2009).

The non-sea-salt sulphates require the prior conversion of SO_2 into sulphuric acid. This oxidation can be performed by several chemical processes, mainly: gaseous oxidation by OH radicals (Seinfeld and Pandis, 2006); aqueous oxidation by oxygen, catalyzed by iron-containing species (Siefert et al., 1996; Deguillaume et al., 2004); aqueous oxidation by ozone and hydrogen peroxide (Keene et al., 1998; Krischke et al., 2000; Rattigan et al., 2000; Hoppel and Caffrey, 2005); and finally heterogeneous oxidation on particle surfaces (Chen et al., 2007). Smectites can provide reactive environments for heterogeneous chemistry under more humid conditions as particles are transported out of the arid source region (Hatch et al., 2007). But the amount of calcium as interlayer cations is limited, and reactions could progress disturbing the octahedral and even tetrahedral sheets of smectites (and occasionally other phyllosilicates) creating complex sulphates (Andreae et al., 1986) and producing amorphous matter (silica and Fe oxides) in advanced stages. Fig. 7A illustrates the case of a neoformed sulphate. We can therefore speculate that the phyllosilicates actually found represent only a remnant of the original quantity.

The larger amounts of amorphous matter, sulphates and smectites in F3 samples (Fig. 3) could indicate that part of the former two would be linked to smectites. TEM observations show that the connection between smectite and sulphate particles is common, but it is difficult to explain the high content of sulphates if we consider only the release of the interlayered Ca of smectites. Their EDX spectra (0.12 atoms of Ca by half-unit cell, on average) suggest, therefore, that an additional process may be the dissolution and rearrangement of original minerals, mainly sulphates (thick band textures, Fig. 7B) and salt (calcite, halite) during tray washing, reinforcing the amount of Ca available from smectites.

Kaolinite is commonly found in these aerosols, but palygorskite (Fig. 2C) is only occasional. Kaolinite evidences that the source areas have undergone intense leaching, typical of tropical lateritic soils. In North Africa, kaolinite distribution is graded by latitude (Paquet et al., 1984; Prospero, 1999) with trace amounts in the northern and westernmost part of North Africa, while it is more common in the central and southern Sahara and abundant in the Sahel and equatorial regions (Caquineau et al., 1998). This indicates that African Sahel soils are a relevant source of our aerosols. Palygorskite is characteristic of the sub-arid belts of the northern hemisphere, whose formation is favoured by evaporation and chemical concentration in poorly drained carbonate rocks in the anti-Atlas (El Mouden et al., 2005). This clay mineral can be distributed by wind over long-range distance as far as northern Europe and has been used to trace the Saharan origin of dust (Molinaroli, 1996).

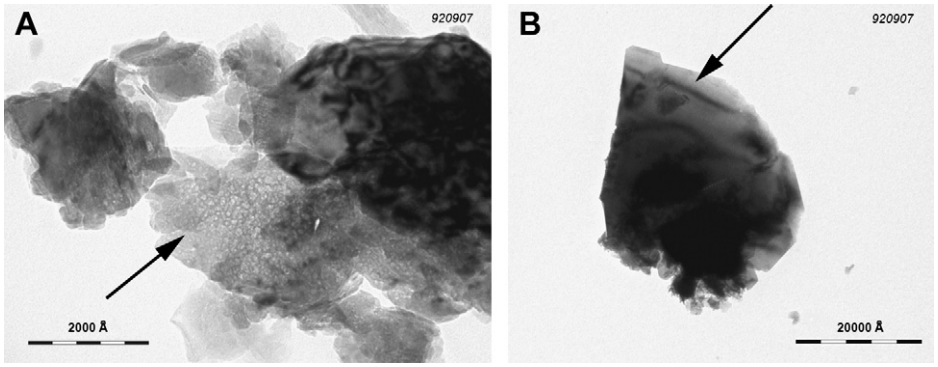

Fig. 7. HRTEM images of some sulphate textures. (A) Textural aspect of neoformed sulphates (arrow) in the air, formed by irregular and small sulphate crystals. (B) Thick bands (arrow) taken on an F3 sample.

It is unusual to find aluminium oxyhydroxides, such as the crystals with hexagonal habit shown in Fig. 2A and B. This is probably an inherited phase, also from source areas with intensively leached soils, and the presence of gibbsite is probable. Gibbsite is often found as part of the structure of clay minerals (illite, kaolinite and smectites) in which the neutral aluminium hydroxide sheets are found sandwiched between silicate sheets. The destruction of these structures can occur either by intense washing over long periods, or by acid attack. This second method implies neoformation processes and could potentially occur in the atmosphere, but the resulting crystals would be poorly arranged and associated with other residual matter (amorphous matter, sulphates), which is not the case here. The degree of conservation of these crystals suggests the washing process and so they would represent an inherited mineral phase.

On the other hand, halite is the main representative mineral of sea salts. The quantities of halite found are high, in spite of the sampling area being relatively far from the sea. This could be related with fronts and precipitation events or indicate passage of the aerosols across the MBL. Occasionally it may be related with other chlorides, such as silvite. The antagonistic relation between quartz and salts (neoformed sulphates and chlorides, Fig. 6) could be due to the physicochemical properties of quartz (inherited mineral) that is not involved in atmospheric heterogeneous reactions; thus, the presence of quartz is an obstacle for the development of processes originating these salts.

Amorphous matter includes a set of heterogeneous dust components such as Fe oxyhydroxides, amorphous silica and organic compounds with low crystallinity and poor diffraction patterns.

Fig. 4 shows the temporal evolution of the deposition rate for major mineral phases. These patterns suggest that the dynamics of mineral supply are governed by the maxima found in the region between the end of February and the end of September (weeks 9 and 38), when the predominant winds are southerly or in some cases westerly. The sinusoidal trace of the annual evolution of major dust constituents defines considerable width between peaks and valleys, whereas minor constituents present a more monotone, parallel evolution.

The predominant minerals (Table 2) in the aerosols collected in the southern Iberian Peninsula were quartz, calcite and dolomite, which together reached an accumulation rate of 11.5 g m^{-2} yr^{-1} (50% of the annual rate); phyllosilicates added up to 6.9 g m^{-2} yr^{-1} (29.9%), of which smectites were the most abundant (2.1 g m^{-2} yr^{-1}, i.e., 9.1%); finally halite and sulphates (salts) respectively contributed 1.8 and 1.3 g m^{-2} yr^{-1} (8.0 and 5.6%).

Reid et al. (2003) found that 70% of all mineral particle mass originating from Africa and collected in the Caribbean area can be attributed to alumino-silicates (probably clay and feldspars). In our case, alumino-silicates represent about 32%, approximately half the amount found in the Caribbean. This discrepancy could be due to size segregation during transport resulting in the preferential deposition of coarser particles (mainly quartz, feldspars and calcite), or to different source areas.

Table 2
Total annual rates according to mineral phases, ordered by decreasing quantities. These values compute the three obtained types of samples (F1 + F2 + F3). Total smectites=smectites 22+17+13. Total sulphates=bassanite+gypsum.

	g m^{-2} yr^{-1}	%		g m^{-2} yr^{-1}	%
Quartz	4.90	21.26	Smectite 22	0.77	3.34
Dolomite	3.36	14.58	Smectite 17	0.73	3.15
Calcite	3.28	14.21	Smectite 13	0.60	2.61
Halite	1.84	7.99	Paragonite	0.52	2.25
Kaolinite	1.82	7.89	Gypsum	0.42	1.82
Illite/Muscovite	1.63	7.06	Feldspars	0.18	0.80
Amorphous	1.15	4.99	Graphite	0.17	0.72
Bassanite	0.86	3.74	*Total smectites*	2.10	9.10
Chlorite	0.82	3.57	*Total sulphates*	1.28	5.56

5. Conclusions

The overall rate of mineral deposition during a year in the southeastern Iberian Peninsula was 26.03 g m^{-2} yr^{-1}, with important maxima mainly in spring and summer. The mineral constituents are as follows (in g m^{-2} yr^{-1}): quartz, 4.90 (21.26%); dolomite, 3.36 (14.58%); calcite, 3.28 (14.21%); smectites, 2.10 (9.10%); halite, 1.84 (7.99%); kaolinite, 1.82 (7.89%); illite/muscovite, 1.63 (7.06%); amorphous matter (iron oxyhydroxides, amorphous silica and organic compounds), 1.15 (4.99%); bassanite, 0.86 (3.75%); chlorite, 0.82 (3.57%); paragonite, 0.52 (2.25%); gypsum, 0.42 (1.82%); feldspars, 0.18 (0.80%); and graphite, 0.17 (0.72%). Trace minerals are palygorskite, apatite, titanium oxides and aluminium oxyhydroxides. Graphite only represents minor quantities.

Most of these minerals are inherited from tropical soils. The sulphates (bassanite and gypsum) are the major neoformed minerals due to heterogeneous multiphase reactions in the atmosphere and have a close relationship ($R = 0.8110$, $p = 0.000$) with phyllosilicates, mainly smectites. The relationships are antagonistic between quartz–halite and smectites, and between calcite–gypsum.

Due to their physicochemical properties, smectites seem to play an essential role in the atmospheric processing of SO_2 and in secondary sulphate genesis.

Acknowledgements

We are grateful to J. Santamarina (Instituto Andaluz de Ciencias de la Tierra, CSIC–UGR) and to M.M. Abad (Centro de Instrumentación Científica, UGR) for their efficient technical assistance. Similarly we are grateful to L. Vágó and D. Lajkó (University of Budapest) for their help on laboratory procedures. We also wish to thank the AEMET (Agencia Estatal de Meteorología, Spain) for meteorological and aerosol data and two anonymous reviewers.

Appendix. Supplementary material

Supplementary data related to this article can be found online at doi:10.1016/j.atmosenv.2011.03.024.

References

Adachi, K., Buseck, P.R., 2008. Internally mixed soot, sulfates and organic matter in aerosol particles from Mexico City. Atmos. Chem. Phys. 8, 6469–6481.
AEMET (Ag Española de Meteorología). Valores climatológicos normales, Granada (Aeropuerto). Available from: http://www.aemet.es.
Alastuey, A., Querol, X., Castillo, S., Escudero, M., Ávila, A., Cuevas, E., Torres, C., Romero, P., Expósito, F., García, O., Díaz, J.P., Dingenen, R., Putaud, J.P., 2005. Characterization of TSP and PM2.5 at Izaña and Sta. Cruz de Tenerife (Canary Islands, Spain) during a Saharan dust episode (July 2002). Atmos. Environ. 39, 4715–4728.
Al-Hosney, H.A., Grassian, V.H., 2004. Carbonic acid: an important intermediate in the surface chemistry of calcium carbonate. J. Am. Chem. Soc. 126, 8068–8069.
Andreae, M.O., Charlson, R.J., Bruynseels, F., Storms, H., Van Grieken, R., Maenhaut, W., 1986. Internal mixture of sea salt, silicates, and excess sulphate in marine aerosol. Science 232, 1620–1623.
Andreae, M.O., 1995. Climate effects of changing atmospheric aerosol levels. In: Hendersson-Sellers, A. (Ed.), World Survey of Climatology. Future Climate of the World, vol. 16. Elsevier Science, New York, pp. 341–392.
Andreae, M.O., 2001. The dark side of aerosols. Nature 409, 671–672.
Ávila, A., Queralt-Mitjans, I., Alarcón, M., 1997. Mineralogical composition of African dust delivered by red rains over Northeastern Spain. J. Geophys. Res. 102D18, 21977–21996.
Ávila, A., Alarcón, M., Queralt-Mitjans, I., 1998. The chemical composition of dust transported in red rains. Its contribution to the biogeochemical cycle of a Holm oak forest in Catalonia (Spain). Atmos. Environ 32, 179–191.
Basma, A.A., Al-Homoud, A.S., Malkawiand, A.I.H., Al-Bashabsheh, M.A., 1996. Swelling–shrinkage behavior of natural expansive clays. App. Clay Sci. 11, 211–227.
Bücher, A., 1994. Ètude en Europe des retombées de poussiéres d'origine saharienne. Rev. Geomorphol. Dyn. 43, 23–25.
Buseck, P.R., Cowley, J.M., Eyring, L. (Eds.), 1988. High Resolution Transmission Electron Microscopy and Associated Techniques. Oxford University Press, New York, p. 645.
Caquineau, S., Gaudichet, A., Gomes, L., Magonthier, M.C., Chatenet, B., 1998. Saharan dust: clay ratio as a relevant tracer to assess the origin of soil-derived aerosols. Geophys. Res. Lett. 25, 983–986.
Carmichael, G.R., Zhang, Y., Chen, L.L., Hong, M.S., Ueda, H., 1996. Seasonal variation of aerosol composition at Cheju Island, Korea. Atmos. Environ. 30, 2047–2416.
Claquin, T., Schulz, M., Balkanski, Y.J., 1999. Modeling the mineralogy of atmospheric dust sources. J. Geophys. Res. 104, 22243–22256.
Coudé-Gaussen, G., Rognon, P., Bergametti, G., Gomes, I., Strauss, B., Gros, J.M., 1987. Saharan dust on the Fuerteventuta island (Canaries): chemical and mineralogical characteristics, air masses trajectories, and probable sources. J. Geophys. Res. 92, 9753–9771.
Chen, H.H., Kong, L.D., Chen, J.M., Zhang, R.Y., Wang, L., 2007. Heterogeneous uptake of carbonyl sulphide on hematite and hematite–NaCl mixtures. Environ. Sci. Technol. 41, 6484–6490.
Chester, R., Johnson, R.L., 1971. Atmospheric dust collected off the Atlantic coasts of North Africa and the Iberian Peninsula. Mar. Geol. 11, 251–260.
Deguillaume, L., Leriche, M., Monod, A., Chaumerliac, N., 2004. The role of transition metals ions on HO_x radicals in clouds: a numerical evaluation of its impact on multiphase chemistry. Atmos. Chem. Phys. 4, 95–110.
Dentener, F.J., Carmichael, G.R., Zhang, Y., Lelieveld, J., Crutzen, P.J., 1996. Role of mineral aerosol as a reactive surface in the global troposphere. J. Geophys. Res. 101, 22869–22889.
Díaz-Hernández, J.L., Miranda, J.M., 1997. Tasas de acumulación de polvo atmosférico en un área semiárida del entorno mediterráneo occidental. Est. Geol. 53, 211–220.
Díaz-Hernández, J.L., Párraga, J., 2008. The nature and formation of iberulites: pinkish mineral microesferulites. Geochim Cosmochim Acta 72, 3883–3906.
Dogan, M., Dogan, A.U., Yesilyurt, F.I., Alaygut, D., Buckner, I., Wurste, D.E., 2007. Baseline studies of the Clay Minerals Society special clays: specific surface area by the Brunauer Emmet Teller (BET) method. Clays Clay Miner. 55, 534–541.
El Mouden, A., Bouchaou, L., Snoussi, M., 2005. Constraints on alluvial clay mineral assemblages in semiarid regions. The Souss Wadi Basin (Morocco, Northwestern Africa). Geol. Acta 3 (1), 3–13.
Falkovich, A., Ganor, E., Levin, Z., Formenti, P., Rudich, Y., 2001. Chemical and mineralogical analysis of individual mineral dust particles. J. Geophys. Res. 106, 18029–18036.
Ganor, E., 1991. The composition of clay minerals transported to Israel as indicator of Saharan dust emission. Atmos. Environ. 25A, 2657–2664.
Ganor, E., Deutsch, Y., Foner, H.A., 2000. Mineralogical composition and sources of airborne settling particles on Lake Kinneret (the Sea of Galilee), Israel. Water Air Soil Poll. 118, 245–262.
Gelencsér, A., 2004. Carbonaceous Aerosol, Atmospheric and Oceanographic Sciences Library, vol. 30. Springer, The Netherlands. 350 p..
Glaccum, R.A., Prospero, J.M., 1980. Saharan aerosols over the tropical North Atlantic – mineralogy. Mar. Geol. 37, 295–321.
Gobbi, G.P., Barnaba, F., Ammannato, L., 2007. Estimating the impact of Saharan dust on the year 2001 PM10 record of Rome, Italy. Atmos. Environ. 41, 261–275.
Goudie, A.S., 2009. Dust storms: recent developments. J. Environ. Manage. 90, 89–94.
Guerzoni, S., Molinaroli, E., Chester, R., 1997. Saharan dust inputs to the western Mediterranean Sea: depositional patterns, geochemistry and sedimentological implications. Deep Sea Res. Part II 44 (3–4), 631–654.
Hatch, C.D., Gough, R.V., Tolbert, M.A., 2007. Heterogeneous uptake of the C1 to C4 organic acids on a swelling clay mineral. Atmos. Chem. Phys. 7, 4445–4458.
Herich, H., Tritscher, T., Wiacek, A., Gysel, M., Weingartner, E., Lohmann, U., Baltensperger, U., Cziczo, D.J., 2009. Water uptake of clay and desert dust aerosol particles at sub- and supersaturated water vapour conditions. Phys. Chem. Chem. Phys. 11, 7804–7809.
Hoppel, W.A., Caffrey, P.F., 2005. Oxidation of S(IV) in sea-salt aerosol at high pH: ozone versus aerobic reaction. J. Geophys. Res.-Atmos. 110, D23202.
IARA-CSIC, 1989. Mapa de suelos de Andalucía E. 1:400.000, 96 p..
IPCC, 2007. Climate change 2007. Synthesis report. In: Core Writing Team, Pachauri, R.K., Reisinger, A. (Eds.), Contribution of Working Groups I, II and III to the Fourth Assessment Report of the Intergovernmental Panel on Climate Change. IPCC, Geneva, Switzerland, p. 104.
Jacob, D.J., 2000. Heterogeneous chemistry and tropospheric ozone. Atmos. Environ. 34, 2131–2159.
Kandler, K., Schütz, L., Deutscher, C., Ebert, M., Hofmann, H., Jäckel, S., Jaenicke, R., Knippertz, P., Lieke, K., Massling, A., Petzold, A., Schladitz, A., Weinzierl, B., Wiedensohler, A., Zorn, S., Weinbruch, S., 2009. Size distribution, mass concentration, chemical and mineralogical composition and derived optical parameters of the boundary layer aerosol at Tinfou, Morocco, during SAMUM 2006. Tellus 61B, 32–50.
Keene, W.C., Sander, R., Pszenny, A.A.P., Vogt, R., Crutzen, P.J., Galloway, J.N., 1998. Aerosol pH in the marine boundary layer: a review and model evaluation. J. Aerosol Sci. 29, 339–356.
Kovács-Kis, V., Pósfai, M., Lábár, J.L., 2006. Nanostructure of atmospheric soot particles. Atmos. Environ. 40, 5533–5542.
Krischke, U., Staubes, R., Brauers, T., Gautrois, M., Burkert, J., Stobener, D., Jaeschke, W., 2000. Removal of SO_2 from the marine boundary layer over the Atlantic Ocean: a case study on the kinetics of the heterogeneous S(IV) oxidation on marine aerosols. J. Geophys. Res.-Atmos. 105, 14413–14422.
Lawrence, C.R., Neff, J.C., 2009. The contemporary physical and chemical flux of Aeolian dust: a synthesis of direct measurements of dust deposition. Chem. Geol. 267, 46–63.
Li, L., Chen, Z.M., Zhang, Y.H., Zhu, T., Li, J.L., Ding, J., 2006. Kinetics and mechanism of heterogeneous oxidation of sulphur dioxide by ozone on surface of calcium carbonate. Atmos. Chem. Phys. 6, 2453–2464.
Loÿe-Pilot, M.D., Martin, J.M., Morelli, J., 1986. Influence of Sahara dust on the rain acidity and atmospheric input to the Mediterranean. Nature 321, 427–428.
Manktelow, P.T., Carslow, K.S., Mann, G.W., Spracklen, D.V., 2010. The impact of dust on sulphate aerosol, CN and CNN during an East Asian dust storm. Atmos. Chem. Phys. 10, 365–382.
Martín-Ramos, J.D., Hidalgo, M.A., Rodríguez-Gallego, M., Otalora, F., 1988. Estudio cristaloquímico de micas de Sierra Nevada. In: Cordillera Bética. II Congreso Geológico de España, Granada, pp. 255–265.
Martín-Ramos, J.D., 2004. Using XPowder – a Sofware Package for Powder X-ray Diffraction Analysis. D.L.GR-1001/04, ISBN 84-609-1497-6 Spain.
Menéndez, I., Díaz-Hernández, J.L., Mangas, J., Alonso, I., Sánchez-Soto, P.J., 2007. Airborne dust accumulation and soil development in the north-east sector of Gran Canaria (Canary Islands, Spain). J. Arid Environ. 71, 57–81.
Meunier, A., 2005. Clays. Springer-Verlag, Berlin, Heidelberg. 472 p..
Middleton, N.J., Goudie, A.S., 2001. Saharan dust, sources and trajectories. Trans. Inst. Br. Geogr. 26, 165–182.
Mills, M.J., Toon, O.B., Thomas, G.E., 2005. Mesospheric sulfate aerosol layer. J. Geophys. Res. 110, D24208.
Molinaroli, E., 1996. Mineralogical characterization of Saharan dust with a view to its final destination in Mediterranean sediments. In: Guerzoni, S., Chester, R. (Eds.), The Impact of Desert Dust Across the Mediterranean. Kluwer Academic, Dordrecht, pp. 153–162.
Munsell Color Company, 1995. Munsell Soil Colour Charts. M.D, Baltimore.
Paquet, H., Coudé-Gaussen, G., Rognon, P., 1984. Étude minéralogique des poussières sahariennes le long d'un itinéraire entre 19° and 35° de latitude Nord. Rev. Geol. Dyn. Geogr. Phys. 25, 257–265.

Prospero, J.M., 1999. Long-range transport of mineral the dust in the global atmosphere: impact of African dust on the environment of the southeastern United States. Proc. Natl. Acad. Sci. U. S. A. 96, 3396–3403.
Prospero, J., Ginoux, P., Torres, O., Nicholson, S.E., 2002. Environmental Characterization of Global sources of atmospheric soil dust derived from the NIMBUS-7 TOMS absorbing aerosol product. Rev. Geophys. 40 (1), 1002.
Rattigan, O.V., Boniface, J., Swartz, E., Davidovits, P., Jayne, J.T., Kolb, C.E., Worsnop, D.R., 2000. Uptake of gas-phase SO_2 in aqueous sulfuric acid: oxidation by H_2O_2, O_3 and HONO. J. Geophys. Res.-Atmos. 105, 29065–29078.
Reid, E.A., Reid, J.S., Meier, M.M., Dunlap, M.R., Cliff, S.S., Broumas, A., Perry, K., Maring, H., 2003. Characterization of African dust transported to Puerto Rico by individual particle and size segregated bulk analysis. J. Geophys. Res. 108 (D19), 8591.
Seinfeld, J.H., Pandis, S.M., 2006. Atmospheric Chemistry and Physics: From Air Pollution to Climate Change. Wiley-Interscience, New York. 1203 p..
Siefert, R.L., Webb, S.M., Hoffman, M.R., 1996. Determination of photochemically available iron in ambient aerosols. J. Geophys. Res.-Atmos. 101, 14441–14450.
Simonson, R.W., 1995. Airborne dust and its significance to soils. Geoderma 65, 1–43.
Tafuro, A.M., Barnaba, F., De Tomasi, F., Perrone, M.R., Gobbi, G.P., 2006. Saharan dust particle properties over the central Mediterranean. Atmos. Res. 81, 67–93.
Tanaka, T.Y., Chiba, M., 2006. A numerical study of the contributions of dust source regions to the global dust budget. Global Planet. Change 52, 88–104.
Tegen, I., Werner, M., Harrison, S.P., Kohfeld, K.E., 2004. Relative importance of climate and land use in determining present and future global soil dust emission. Geophys. Res. Lett. 31, L05105.
Ullerstam, M., Johnson, M.S., Vogt, R., Ljungström, E., 2003. DRIFTS and Knudsen cell study of the heterogeneous reactivity of SO_2 and NO_2 on mineral dust. Atmos. Chem. Phys. 3, 2043–2051. http://www.atmos-chem-phys.net/3/2043/2003/.
Ullerstam, M., Vogt, R., Langer, S., Ljungström, E., 2002. The kinetics and mechanism of SO_2 oxidation by O_3 on mineral dust. Phys. Chem. Chem. Phys. 4, 4694–4699.
Usher, C.R., Al-Hosney, H., Carlos-Cuellar, S., Grassian, V.H., 2002. A laboratory study of the heterogeneous uptake and oxidation of sulphur dioxide on mineral dust particles. J. Geophys. Res.-Atmos. 107, 4713–4722.
Zhang, D.Z., Shi, G.Y., Iwasaka, Y., Hu, M., 2000. Mixture of sulphate and nitrate in coastal atmospheric aerosols: individual particle studies in Quingdao (36° 04′ N, 120° 21′ E), China. Atmos. Environ. 34, 2669–2679.
Zhuang, H.C., Chan, C.K., Fang, M., Wexler, A.C., 1999. Formation of nitrate and non-sea-salt sulphate on coarse particles. Atmos. Environ. 33, 4223–4233.